JOURNAL OF MATERIALS SCIENCE **38** (2003) 2893–2899

Zinc hydroxystannate-coated metal hydroxide fire retardants: Fire performance and substrate-coating interactions

P. R. HORNSBY
Wolfson Centre for Materials Processing, Brunel University, Uxbridge, Middlesex, UB8 3PH, UK

P. A. CUSACK, M. CROSS
Tin Technology Limited, Kingston Lane, Uxbridge, Middlesex, UB8 3PJ, UK

A. TÓTH, B. ZELEI
Research Laboratory of Materials and Environmental Chemistry, Chemical Research Center of the Hungarian Academy of Sciences, H-1525 Budapest, P.O.B. 17, Hungary

G. MAROSI
Department of Organic Chemical Technology, Budapest University of Technology and Economics, H-1521 Budapest, P.O.B. 91, Hungary

Fire retardant (FR) properties, including limiting oxygen index, peak rate of heat release and smoke parameter have been measured and compared for unfilled and filled polyvinyl-chloride (PVC) based cable formulations, containing various amounts of uncoated and zinc-hydroxystannate (ZHS)-coated alumina trihydrate (ATH) and magnesium hydroxide (MH) fillers. Uncoated ATH or MH proved to be efficient FR additives, but when coated with ZHS, further improvements were observed. ATH was more effective than MH in both uncoated and ZHS-coated forms. For a halogen-free ethylene-vinyl acetate (EVA) cable formulation, the content of vinyl acetate and loading of ZHS-coated ATH required to yield optimum FR properties was determined. The interaction between ATH substrate and ZHS coating was also studied by X-ray photoelectron spectroscopy and diffuse reflectance infrared Fourier-transform spectroscopy, using samples with ZHS-contents ranging from 1 to 15 wt%. An increase in the binding energies of the Zn $2p_{3/2}$ and Sn $3d_{5/2}$ peaks was found, together with alterations in the positions of the (Sn)O–H stretching bands. There was no evidence for condensation and the formation of Al–O–Sn bonds.

Introduction

Zinc hydroxystannate ($Zn[Sn(OH)_6]$, ZHS)-coated fillers are novel fire retardant and smoke suppressant additives for polymeric materials. The application of a ZHS coating to various hydrated inorganic fillers, in particular aluminium hydroxide and magnesium hydroxide, allows a significant reduction to be made to the overall filler loading, with no loss in fire retardant properties [1–7].

In this paper we evaluate the fire retardant behaviour of these systems in typical PVC and EVA cable formulations. In addition, the filler-coating interaction is studied in the ZHS-coated ATH system by X-ray photoelectron spectroscopy (XPS or ESCA) and diffuse reflectance infrared Fourier-transform (DRIFT) spectroscopy.

Experimental

Sample preparation

ZHS-coated fillers were prepared in the following manner. 1000 g of alumina trihydroxide (ATH, Alcan SF4, produced by Alcan Chemicals, UK) was slurried in 8 litres of an aqueous solution containing 103g sodium hydroxystannate. One litre of an aqueous solution, containing 53g zinc chloride, was added dropwise into the slurry, and the resulting mixture stirred for 2 h. The resulting solid product was separated from the solution by centrifugation, washed three times with distilled water and dried in air at 110°C. The dried cake was crushed using a pestle and mortar to give 1,110g of a fine white powder (ZHS-coated ATH). ZHS-coated magnesium hydroxide (MH, Magnifin H5, produced by Martinswerk

AG, Germany) powders were prepared using a similar method.

ZHS-coated ATH and MH fillers were incorporated into a flexible PVC cable formulation with the following composition (in parts by weight):

PVC resin (Vinoflex S, BASF)	100
Plasticiser (dioctyl phthalate)	35
Stabiliser (beta-aminocrotonate, Lonza)	2
Inorganic fillers	0–50

Compositions were firstly melt compounded on a two-roll mill at 175°C, then compression moulded at 170°C for 5 min using an applied pressure of 31 MPa.

ZHS-coated ATH fillers were also incorporated into a halogen-free EVA (ethylene-vinyl acetate) cable formulation. The EVA grades used were Escorene Ultra (Exxon Chemicals), which contained 12%, 19% or 27% of vinyl acetate. Powdered additives were incorporated into the EVA formulations by compounding on a 16 mm twin-screw extruder operating at 155–165°C, followed by compression moulding for 15 min at a pressure of 31 MPa and a temperature of 160°C.

Elemental bulk analysis

ZHS-coated fillers were dissolved in dilute hydrochloric acid, and tin and zinc contents determined using a Liberty 220 Inductively Coupled Plasma Atomic Emission Spectrometer.

BET surface area

Surface areas of the coated fillers were determined by the BET nitrogen absorption technique using a Micromeritics Gemini 2360 BET analyser.

Fire-retardant evaluation

Flame-retardant and smoke-suppressing properties of the PVC and EVA formulations were assessed using two standard fire test techniques: Limiting Oxygen Index and Cone Calorimeter.

The *Limiting Oxygen Index* (LOI) test is an indicator of ease of combustion in an oxygen/nitrogen atmosphere through downward burning of a vertically mounted specimen. The test method is generally reproducible to an accuracy of ±0.5%, giving a useful comparison of the relative flammability of different materials. Higher LOI values represent better flame retardancy. Measurements were undertaken in accordance with BS 2782 (Part 1, Method 141).

The *Cone Calorimeter* uses a truncated conical heater element to irradiate test specimens at heat fluxes from 10 to 100 kW/m^2, thereby simulating a range of fire intensities. The technique has been shown to provide data that correlate well with those from full-scale fire tests. Cone Calorimeter tests were carried out in duplicate, using a 50 kW/m^2 incident heat flux, following procedures recommended in BS 476 (Part 15). The technique provides detailed information about ignition behaviour, heat release and smoke evolution during sustained combustion. The two parameters determined are defined below:

Peak Rate of Heat Release, Peak RHR (kW/m^2)—taken as the peak value of the heat release rate versus time curve, and considered to be the variable that best expresses the maximum intensity of a fire, indicating the rate and extent of fire spread.

Smoke Parameter, SP (MW/kg)—defined as the product of the measured specific extinction area and Peak RHR, this parameter is indicative of the amount of smoke generated in a full-scale fire situation.

XPS measurements

XPS measurements were performed on a Kratos XSAM 800 spectrometer using Mg K$\alpha_{1,2}$ radiation in fixed analyser transmission mode, with 80 and 40 eV pass energy for the wide scan and the detailed spectra, respectively. The samples were mounted on stainless steel sample holders using double-sided adhesive tape. The pressure in the sample analysis chamber was lower than 10^{-7} Pa. The spectra were referenced to the C 1s line of the CH_x type carbon, set to a binding energy of 285 eV. Data acquisition was undertaken with Kratos Vision 2000 software. Data processing, including quantification, was carried out using the recently developed XPS MultiQuant program [8, 9]. The relative differential subshell photoionisation cross-sections were taken from the paper published by Evans *et al*. [10]. The inelastic mean free path values of the photoelectrons were calculated by the method of Seah and Dench [11].

DRIFT measurements

For DRIFT spectroscopic measurements, the samples were mixed with KBr powder in a 4.96 weight ratio of filler:KBr. The spectra were recorded on a Perkin-Elmer 1710 FT-IR spectrophotometer. 200 scans were accumulated in the 4400–400 cm^{-1} wavenumber region at a resolution of 4 cm^{-1}. Each spectrum was subjected to the Kubelka-Munk transformation.

Results and discussion

Fire retardant properties

Table I compares the fire retardant (FR) effect of uncoated and ZHS-coated ATH and MH additives in typical PVC cable formulations.

It can be seen from the improvement of the reported LOI, Peak RHR and SP data that the metal hydroxides,

TABLE I Fire-retardant data for PVC cable formulations

Sample*	LOI	Peak RHR (kW/m^2)	SP (MW/kg)
Control	25.4	239	210
20% ATH	28.5	173	133
50% ATH	33.5	104	20
20% ZHS-coated ATH	36.7	146	51
50% ZHS-coated ATH	45.8	96	27
20% MH	26.8	220	120
50% MH	28.4	207	79
20% ZHS-coated MH	28.8	182	70
50% ZHS-coated MH	33.9	162	40

*All coated fillers contain 10% by weight of ZHS coating.

TABLE II Fire-retardant data for EVA cable formulations

Vinyl acetate content of EVA (%)	Filler (100 phr level)	Peak RHR (kW/m^2)	SP (MW/kg)
12	1% ZHS-coated ATH	465	140
12	10% ZHS-coated ATH	447	144
12	15% ZHS-coated ATH	458	157
19	1% ZHS-coated ATH	461	160
19	10% ZHS-coated ATH	481	157
19	15% ZHS-coated ATH	459	165
27	ATH	472	177
27	1% ZHS-coated ATH	441	151
27	10% ZHS-coated ATH	372	121
27	15% ZHS-coated ATH	426	148

ATH and MH, are in themselves efficient fire retardants. However, the application of a ZHS coating give further improvements to the FR properties of the PVC formulations. In the composition range studied, ATH is a more efficient fire retardant than MH, in terms of improvements to LOI, Peak RHR and SP. (The only exception is the SP of the 20% metal hydroxide-containing PVC samples, for which MH gave a slightly better performance than ATH).

Table II shows the result of cone calorimeter tests for the various halogen-free EVA cable formulations tested at a 50 kW/m^2 irradiance level. It is evident that optimum flame-retardant and smoke-suppressant properties are achieved in the EVA sample containing 27% vinyl acetate and 10% ZHS-coated ATH filler.

Filler/coating interactions

Further detailed investigations were directed towards the ZHS-coated ATH fillers themselves. To this end a series of ATH samples with ZHS-content ranging from 1 to 15% were prepared for investigation. Firstly the bulk composition and surface area of these filler samples was determined, then the interaction between the ZHS-coating and the ATH substrate studied by surface analysis.

TABLE III Bulk analytical data for ZHS-coated ATH samples

	Tin content (%)		Zinc content (%)	
Sample	Calculated	Found	Calculated	Found
1% ZHS on ATH	0.4	0.4	0.2	0.2
2% ZHS on ATH	0.8	0.8	0.5	0.4
3% ZHS on ATH	1.2	1.2	0.7	0.6
4% ZHS on ATH	1.7	1.7	0.9	0.9
5% ZHS on ATH	2.1	2.0	1.1	1.1
10% ZHS on ATH	4.1	4.0	2.3	2.2
15% ZHS on ATH	6.2	6.1	3.4	3.2

TABLE IV BET surface area data for ZHS-coated ATH samples

Sample	BET area (m^2/g) single point determination	BET area (m^2/g) multipoint determination
ATH (uncoated)	6.1	6.2
1% ZHS on ATH	6.0	6.0
2% ZHS on ATH	7.2	7.3
3% ZHS on ATH	5.8	5.9
4% ZHS on ATH	5.2	5.2
5% ZHS on ATH	6.0	6.0
10% ZHS on ATH	7.8	8.0
15% ZHS on ATH	7.5	7.6
ZHS (commercial)	14.7	15.1

Bulk analysis

Table III shows the measured tin- and zinc-content of the ZHS-coated ATH samples and the corresponding calculated values from ZHS applied during the coating procedure.

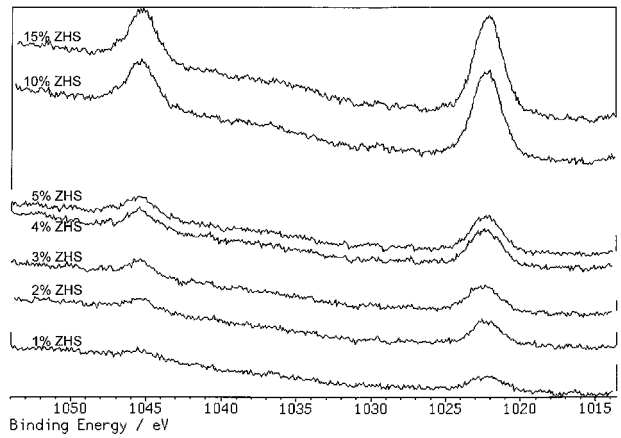

Figure 1 Zn 2p doublet of the ZHS-coated ATH samples.

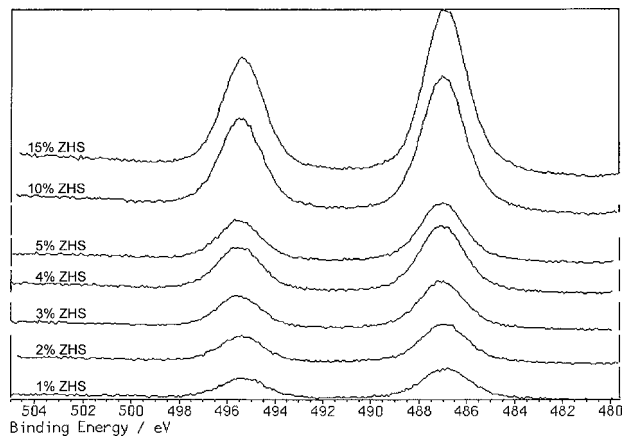

Figure 2 Sn 3d doublet of the ZHS-coated ATH samples.

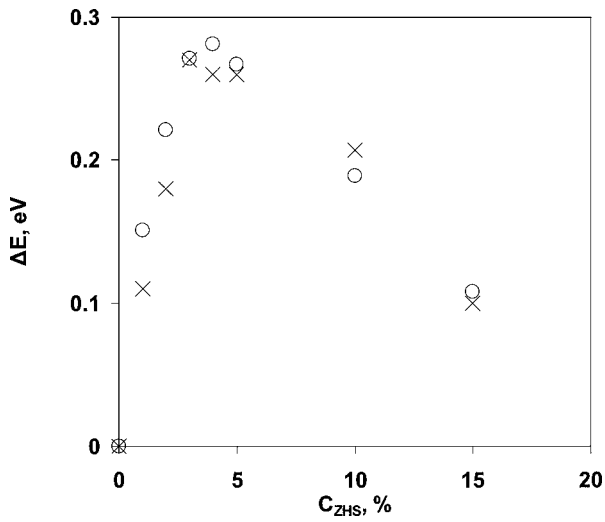

Figure 3 Dependence of the chemical shift on the applied concentration of ZHS (○ Zn $2p_{3/2}$, ♀ Sn $3d_{5/2}$).

As seen in Table III, there is good agreement between the calculated and measured bulk analytical data. Furthermore, tin/zinc mass ratios close to 1.82 were calculated, which is the stoichiometric value expected for $Zn[Sn(OH)_6]$.

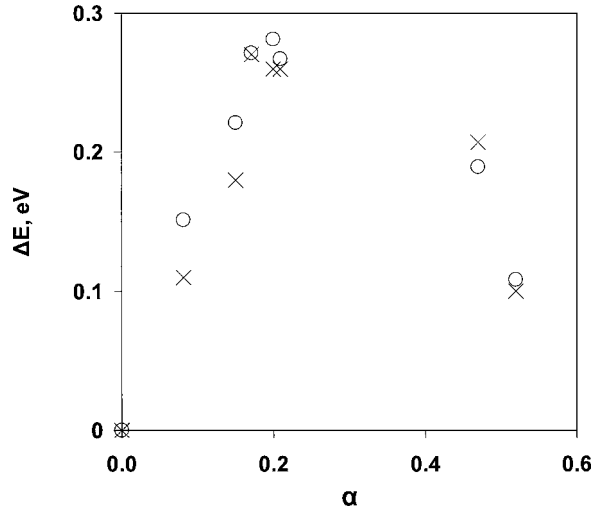

Figure 4 Dependence of the chemical shift on the surface coverage of ATH by ZHS (○ Zn $2p_{3/2}$, ♀ Sn $3d_{5/2}$).

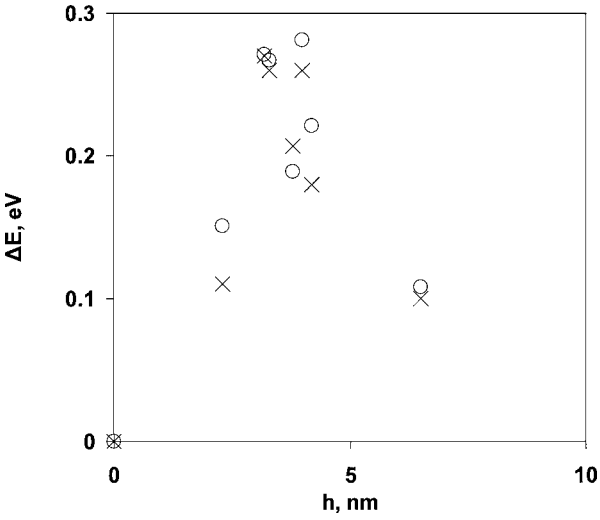

Figure 5 Dependence of the chemical shift on the thickness of the ZHS islands (○ Zn $2p_{3/2}$, ♀ Sn $3d_{5/2}$).

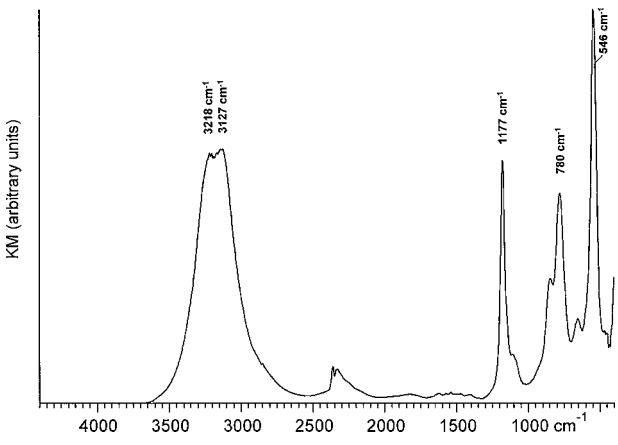

Figure 6 DRIFT spectrum of ZHS.

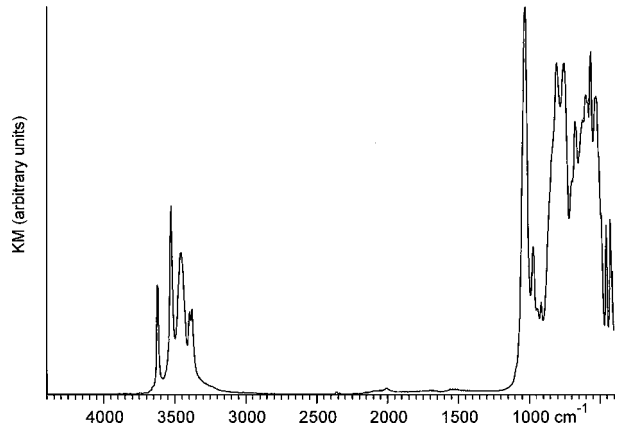

Figure 7 DRIFT spectrum of ATH.

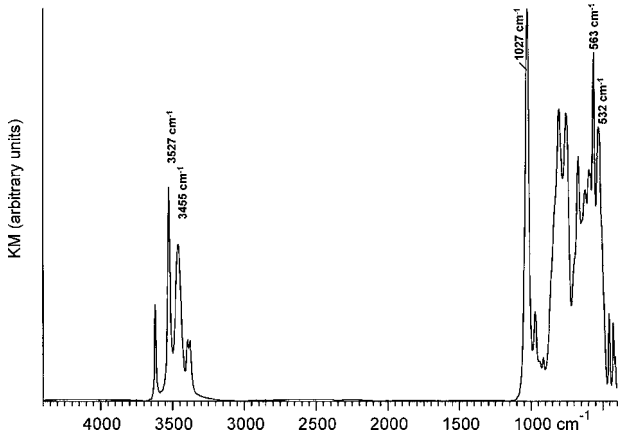

Figure 8 DRIFT spectrum of ATH containing 1% of ZHS.

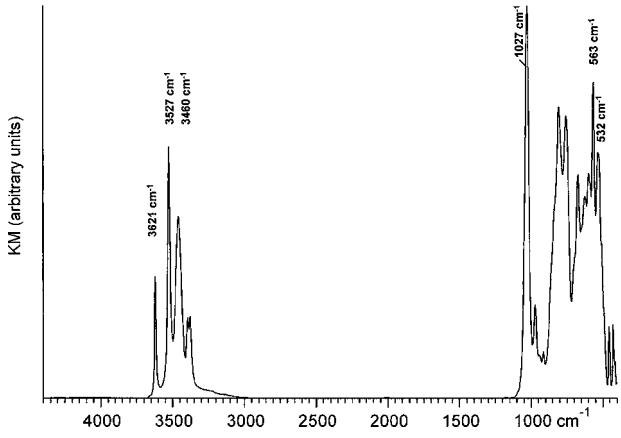

Figure 9 DRIFT spectrum of ATH containing 5% of ZHS.

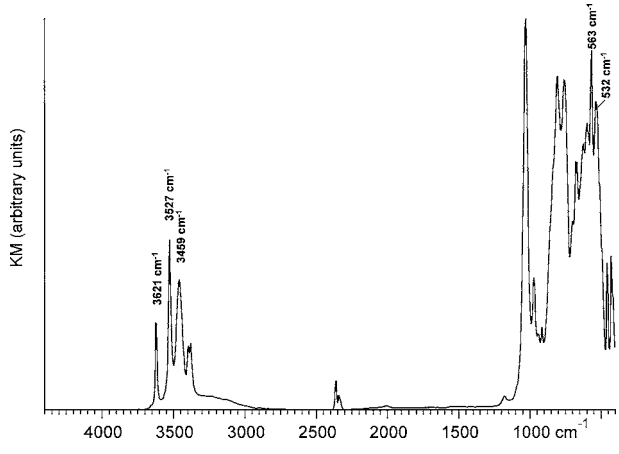

Figure 10 DRIFT spectrum of ATH containing 10% of ZHS.

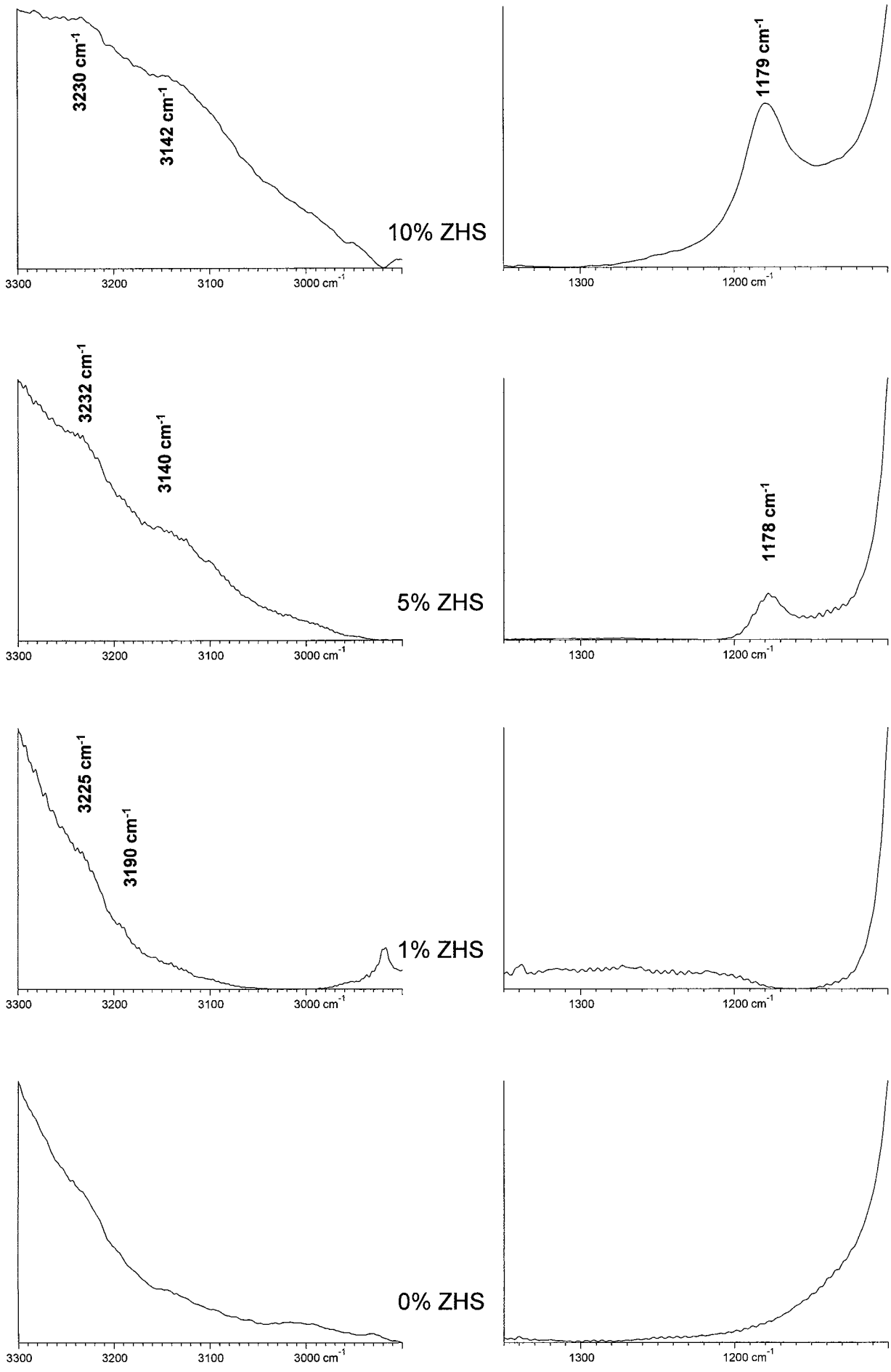

Figure 11 Selected DRIFT spectral regions of ATH and ZHS-coated ATH samples.

Surface area determination

In Table IV the surface area data are compared for pure ATH, ZHS, and for ATH samples coated by ZHS in concentrations ranging from 1% to 15%.

It can be seen that although coating of ATH by ZHS induces some alterations in the surface area ($A = 6.6 \pm 1.4$ m^2/g), these yield no obvious trend.

Surface analysis by XPS

Figs 1 and 2 show the detailed Zn 2p and the Sn 3d regions of the ZHS-coated ATH samples listed in Table III. Zn and Sn can be clearly detected already in case of only 1% of ZHS on ATH. Upon increasing the applied concentration of ZHS, the intensities of the Sn 3d and Zn 2p doublet peaks increase.

Binding energy (BE) values of the Zn $2p_{3/2}$ and Sn $3d_{5/2}$ peaks measured for pure ZHS are 1022.05 eV and 486.8 eV, respectively. Upon coating of ATH by ZHS, these BE values increase, suggesting an interaction between the substrate and the coating. Fig. 3 shows the dependence of the chemical shifts (ΔE) for these lines as a function of the applied concentration of ZHS (c_{ZHS}). According to this figure, in the low c_{ZHS} range ΔE increases with c_{ZHS} for both lines, while after a local maximum at about 4% it decreases.

In a previous paper [12] we found relationships between various parameters, including the concentration of ZHS, surface coverage of ATH by ZHS (α) and thickness of the islands of ZHS (h). It is noteworthy that in the $c_{ZHS} = 1\%$ to 15% interval h was found to be in the low nanometre range, while α varied between about 0.1 and 0.5. Also, h increased with the increase of α from about $3a$ to about $8a$, where a is the lattice parameter of ZHS. Substituting in Fig. 3, the applied c_{ZHS} values with the corresponding values of α or h, the dependence of ΔE of the Zn $2p_{3/2}$ and Sn $3d_{5/2}$ peaks on α or h can be depicted (Figs 4 and 5). According to these figures, the local maximum of ΔE is at about $\alpha = 0.2$ or $h = 4$ nm. The latter value corresponds to a thickness of five lattice parameters [12].

The decreasing part of the curves in Figs 3–5 is reasonable. It can be explained by the increase in h, since the latter implies the increase of the portion of ZHS non-interacting with ATH, and this is expected to result in an asymptotic approach of ΔE to zero. The increasing part of ΔE, however, is unexpected. A possible explanation for this observation is the dependence of the electronic structure and reactivity of nanoclusters on their size and shape [13].

Surface analysis by DRIFT

The DRIFT spectra of the pure ZHS and ATH samples are depicted in Figs 6 and 7, while those of the coated ATH samples containing 1, 5 and 10% of ZHS are shown in Figs 8–10, respectively. In Fig. 11 selected scaled-up regions of ATH and ZHS-coated ATH samples are displayed.

The spectrum of ZHS (Fig. 6) is in agreement with the infrared data published previously [14]. It shows the presence of significant amount of OH groups (3127 and 3218 cm^{-1}, doublet of (Sn)O─H stretching; 1177 cm^{-1} (Sn)O─H in-plane bending). Traces of hydrocarbons are evident (2870 and 2930 cm^{-1}). The doublet at 2331 and 2360 cm^{-1} can be assigned to CO_2 in the air, but the broad band below it indicates the presence of chemisorbed CO_2. The bands at 780 and 546 cm^{-1} may pertain to SnO and ZnO stretching, respectively [14].

The spectrum of ATH (Fig. 7) is in agreement with the IR-spectrum published for gibbsite [15, 16], which is known to have a hydrogen-bonded layer structure. The observed spectrum contains sharp lines, suggesting that the sample is highly-crystalline.

The spectrum of ATH containing 1% of ZHS-coating does not show a clear presence of the ZHS.

The spectrum of ATH containing 5% of ZHS-coating clearly shows the presence of a ZHS phase. In Fig. 11:

- the stretching bands of (Sn)O─H are observed at 3140 and 3232 cm^{-1},
- the in-plane bending of (Sn)O─H is detected at 1178 cm^{-1} and
- the interlayer (Al)OH stretching band became sharper and its maximum was shifted from 3455 cm^{-1} to 3460 cm^{-1}.

In the spectra of ATH containing 10% of ZHS coating (Figs 10 and 11) bands of both ATH and ZHS are clearly seen. ZHS has bands at:

- 3142 and 3230 cm^{-1} (doublet of (Sn)O─H stretching) and
- 1179 cm^{-1} (in-plane bending of (Sn)-O─H.

Conclusions

The chemical shifts for the Zn $2p_{3/2}$ and Sn $3d_{5/2}$ lines, together with alterations in the positions of the (Sn)O─H stretching bands, confirm the interaction between the ATH substrate and the ZHS coating. The lack of a radical decrease in the intensities of the OH-bands suggests that substantial condensation between ATH and ZHS did not occur. This view is further supported by the absence of Al─O─Sn bonds, which would have resulted in the appearance of new stretching bands, probably at about 620 cm^{-1}.

Acknowledgement

This work was supported by the Commission of the European Communities (FP5 GROWTH Programme, Research Project "FLAMERET, New Surface Modified Flame Retarded Polymeric Systems to Improve Safety in Transportation and Other Areas", Contract Number G5RD-CT-1999-00120). One of the authors, Matthew Cross was funded through the EPSRC EngD programme in Environmental Technology at Brunel University.

References

1. P. A. CUSACK, B. PATEL, M. S. HEER and R. G. BAGGALEY, Intern. Patent Appl. PCT/GB96/01475 (1996).
2. R. G. BAGGALEY, P. R. HORNSBY, R. YAHYA, P. A. CUSACK and A. W. MONK, *Fire & Mater.* **21** (1997) 179.

3. P. A. CUSACK and P. R. HORNSBY, *Journal of Vinyl & Additive Technology* **5** (1999) 21.
4. F. LE LAY and J. GUITERREZ, *Polym. Degrad. Stab.* **64** (1999) 397.
5. E. KICKO-WALCZAK, *Polym. Degrad. Stab.* **64** (1999) 439.
6. P. A. ATKINSON, P. J. HAINES and G. A. SKINNER, *Thermochim. Acta* **360** (2000) 29.
7. *Idem.*, *Polym. Degrad. Stab.* **71** (2001) 351.
8. M. MOHAI, *XPS* MultiQuant for Windows, version 1.2. User's Manual. 1999–2001.
9. http://www.chemres.hu/AKKL/index.html
10. S. EVANS, R. G. PRITCHARD and J. M. THOMAS, *J. Electron Spectrosc. Relat. Phenom.* **14** (1978) 341.
11. M. P. SEAH and W. A. DENCH, *Surf. Interface Anal.* **1** (1979) 2.
12. M. MOHAI, A. TÓTH, P. R. HORNSBY, P. A. CUSACK, M. CROSS and G. MAROSI, *Surf. Interface Anal.* (in press).
13. G. A. SOMORJAI and Y.G. BORODKO, *Catal. Letters* **76** (2001) 1.
14. T. DUPUIS, C. DUVAL and J. LECOMTE, *Compt. Rend.* **257** (1963) 3080.
15. R. L. FROST, J. T. KLOPROGGE, S. C. RUSSELL and J. F. SZETU, *Appl. Spectrosc.* **53** (1999) 423.
16. V. C. FARMER (ed.), "The Infrared Spectra of Minerals" (Mineralogical Society, London, 1974) p. 149.

Received 2 August 2002
and accepted 3 April 2003